Applied Microbiology and Biotechnology (2024) 108:503
https://doi.org/10.1007/s00253-024-13342-9

APPLIED GENETICS AND MOLECULAR BIOTECHNOLOGY

A yeast surface display platform for screening of non-enzymatic protein secretion in *Kluyveromyces lactis*

Jiyi An[1,2] · Na Shang[2,3] · Wenting Liu[2,3] · Yuanyuan Niu[2,3] · Qingling Liang[2,3] · Juquan Jiang[1] · Yingying Zheng[2,3]

Received: 4 May 2024 / Revised: 23 September 2024 / Accepted: 22 October 2024 / Published online: 5 November 2024

Abstract

Enhancing the secretion of recombinant proteins, particularly non-enzymatic proteins that predominate in food and pharmaceutic protein products, remains a significant challenge due to limitations in high-throughput screening methods. This study addresses this bottleneck by establishing a yeast surface display system in the food-grade microorganism *Kluyveromyces lactis*, enabling efficient display of model target proteins on the yeast cell surface. To assess its potential as a universal high-throughput screening tool for enhanced non-enzymatic protein secretion, we evaluated the consistency between protein display levels and secretion efficiency under the influence of various genetic factors. Our results revealed a strong correlation between these two properties. Furthermore, screening in a random mutagenesis library successfully identified a mutant with improved secretion. These findings demonstrate the potential of the *K. lactis* surface display system as a powerful and universal tool for high-throughput screening of strains with superior non-enzymatic protein secretion capacity. We believe this study could pave the way for efficient large-scale production of heterologous food and therapeutic proteins in industries.

Key points

- *A YSD (yeast surface display) system was established in Kluyveromyces lactis*
- *This system enables high-throughput screening of non-enzymatic protein secretion*
- *This technology assists industrial production of food and therapeutic proteins*

Keywords *Kluyveromyces lactis* · Yeast surface display · Flow cytometry · High-throughput screening · Secretion · Non-enzymatic proteins

Introduction

Proteins and peptides are essential products in food and pharmaceutical industries. From enzymes in food processing to antibodies in medicine, these biomolecules underpin countless applications. While food enzymes have long been a cornerstone of traditional food processing, the growing health industry has made non-enzymatic proteins essential ingredients in both food and pharmaceutical fields (Tang et al. 2024; Wang et al. 2022; Zeng et al. 2022). Popular examples include therapeutic proteins like lactoferrin, insulin, and interferon, as well as functional food ingredients like osteopontin in baby formula, hemoglobin in "artificial meat," and collagen in health products. However, the production of these valuable proteins often faces challenges, such as scarcity in natural sources and complex extraction processes. To address these limitations, heterologous protein production using food-grade microorganisms offers a safe and promising alternative technology. Secretory expression,

Jiyi An, Na Shang, and Wenting Liu contributed equally.

✉ Juquan Jiang
jjqdainty@163.com

✉ Yingying Zheng
zheng_yy@tib.cas.cn

[1] Department of Microbiology and Biotechnology, College of Life Sciences, Northeast Agricultural University, No. 600 Changjiang Road, Xiangfang District, Harbin 150030, China

[2] Department of Strategic and Integrative Research, Tianjin Institute of Industrial Biotechnology, Chinese Academy of Sciences, Tianjin 300308, China

[3] National Center of Technology Innovation for Synthetic Biology, Tianjin 300308, China

particularly in large-scale industrial processes, is favored due to its cost-effectiveness and ease of purification. For optimal production levels and cost efficiency, selecting the most suitable host organism and implementing high-throughput screening (HTS) for high protein secretion are two critical procedures.

Among commonly used expression hosts, yeasts are a prominent choice for producing recombinant proteins in food and pharmaceutical industries due to their robust post-translational modification capabilities, efficient secretory capacity, rapid growth to high density, and ease of genetic manipulation (Madhavan et al. 2021). While *Saccharomyces cerevisiae* and *Komagataella phaffii* have dominated in bulk industrial enzyme production, they also have drawbacks, such as hyperglycosylation in *S. cerevisiae* and hazardous methanol-based fermentation in *K. phaffii*. A nontraditional yeast, *Kluyveromyces lactis*, offers a promising alternative due to its unique advantages. *K. lactis*, also known as dairy yeast, is the second yeast species approved the Generally Regarded As Safe (GRAS) status for food additives (Almeida et al. 2015). *K. lactis* has been extensively studied from the early 1960s and has a well-established track record of safe applications in food industry, especially in dairy products (Freitas et al. 2020). It can utilize lactose from discarded whey wastes to produce valuable edible cellular biomass in the food industry (Sampaio et al. 2020). Lactase produced by *K. lactis* have been used to produce low-lactose milk for lactose-intolerant individuals. Significantly, *K. lactis* has been established as a robust protein expression system (commercially available kits from NEB, England), facilitating the successful expression of hundreds of heterologous proteins (Fukuhara 2006; Rodicio and Heinisch 2013; Spohner et al. 2016; van Ooyen et al. 2006). The *K. lactis* expression system presents several advantages over traditional yeast hosts, such as high fermentation efficiency due to negative Crabtree effect, high yields of secretion, particularly well-suited for high molecular weight proteins, safer production that is free of methanol and explosion-proof devices, and proper glycosylation (van den Dungen et al. 2021; Rodicio et al. 2022). A significant number of pharmaceutical proteins have been successfully produced in *K. lactis*, such as interferon-α (Kumar et al. 2005; Musch et al. 2004), macrophage colony-stimulating factor (M-CSF) (Hua et al. 1994), insulin precursors (Feng et al. 1997), and various antibodies (Legastelois et al. 2017; Robin et al. 2003; Swennen et al. 2002). The recombinant bovine chymosin produced by DSM Corporation using *K. lactis* holds a significant share of the global market. However, some challenges, especially the low secretion levels for certain proteins, still need to be addressed.

Significant efforts continue to enhance the secretory expression of heterologous protein in yeasts. These studies explore the combined approach of rational design and random mutagenesis, targeting both chassis cell modification and the development of powerful genetic elements (Idiris et al. 2010). However, identifying strains with superior non-enzymatic protein secretion remains a bottleneck due to limitations in HTS methods. Consequently, the screening has to be carried out in a relatively small library based on protein electrophoresis detection. Another alternative approach is to fuse non-enzymes to reporter proteins like enzymes or fluorescent proteins for high-throughput detection (Cong et al. 2022). Droplet-based microfluidics technology can improve screening efficiency but requires a unique and complex water/oil microencapsulation protocol for each individual protein and costly fluorescent substrates (Stucki et al. 2021). In addition, reporter parts can potentially impact secretion levels, leading to screening failure (Yang et al. 2016). Given that non-enzymatic proteins constitute the majority of food and pharmaceutical proteins, more effective and reliable HTS methods are urgently needed to rapidly identify high-producing clones from expanding mutant libraries containing synergistic secretion factors.

Yeast surface display (YSD) is a technique for the expression, secretion, and immobilization of heterologous target proteins (TPs) on the yeasts' cell surface by fusing them to the cell wall proteins (CWPs) or anchor domains (Teymennet-Ramírez et al. 2022) (Fig. 1b). The anchor-fused TPs experience the same trafficking process as the secretory proteins. In previous study, Shusta et al. (1999) demonstrated a correlation between YSD display levels and actual protein secretion in their system. Therefore, in these cases, in combination with immunofluorescence labelling, flow cytometry analysis, and fluorescence-activated cell sorting (FACS) techniques for visual measurement and cell sorting, YSD has the potential to serve as an alternative HTS method for identifying high-secretory clones. The most critical genetic part affecting YSD efficiency is anchors (Teymennet-Ramírez et al. 2022). Among these, GPI (glycosylphosphatidylinositol)-CWP anchors are particularly favored due to their broad applicability across various yeast species (Tanaka and Kondo 2014; Yang et al. 2019; Zhao et al. 2017). Prominent examples of GPI-CWP anchors include a-agglutinin (Aga1-Aga2), α-agglutinin, flo1 (flocculin), and sed1 (stress-induced cell wall structural protein), especially in *S. cerevisiae*, *K. phaffii*, and *Yarrowia lipolytica*. The identification of optimal anchor sequences in other yeast species is an ongoing area of research (Cheon et al. 2014). To our knowledge, YSD system has not been established in *K. lactis.* The only reported protein expression on cell surface of *K. lactis* is anchored to plasma membrane using a mouse CWP, which is totally different from other traditional YSD systems and far from optimized (Uccelletti et al. 2002).

This study established an efficient YSD system in *K. lactis*. *Homo sapiens* interleukin 1β (IL-1β) and human serum

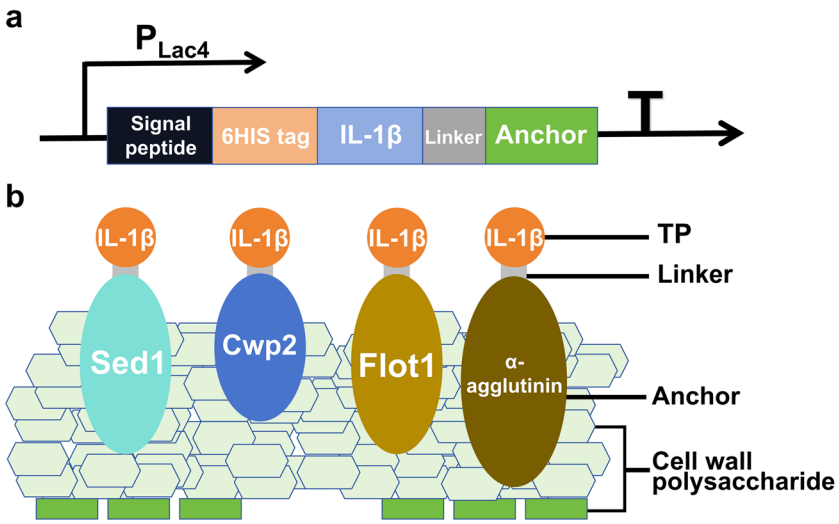

Fig. 1 Construction of YSD system in *K. lactis*. **a** Expression cassettes of YSD system in *K. lactis*. **b** Schematic representation of IL-1β displaying on the cell surface of *K. lactis* through different anchors

albumin (HSA), as two non-enzymatic TP models known for their complex structures and low secretory efficiencies in *K. lactis* (Bao and Fukuhara 2001), were successfully displayed on the *K. lactis* cell surface. Our further findings demonstrated the feasibility and reliability of employing this YSD system as a HTS method for identifying potent genetic elements and chassis strains that enhance recombinant non-enzyme secretion in *K. lactis*. This work lays the foundation for diverse applications of YSD technology in *K. lactis*, particularly as a powerful HTS method for identifying strains with superior non-enzymatic protein secretion capacity.

Materials and methods

Strains, plasmids, and cultivation condition

Escherichia coli DH5α was used for cloning experiments. *E. coli* was cultured at 37 °C in LB medium (0.5% yeast extract, 1% tryptone, 1% NaCl). *K. lactis* GG799 (New England BioLabs Inc., Ipswich, MA; wild-type genotype) was used to construct YSD and secretory strains. *K. lactis* was cultured at 30 °C in YPG medium (2% peptone, 1% yeast extract, 2% galactose). The expression cassettes of secreted or displayed TPs were cloned into the shuttle plasmid pKLAC1 (NEB, Ipswich, MA), which contains an *Amds* gene allowing recombinants to utilize acetamide as the sole nitrogen source upon co-integration with the TP gene. Yeast transformants were screened and cultured on YCBAg agar plates (Yeast Carbon Base medium supplemented with 5 mM acetamide, 2% galactose, and 1.5% agar).

Plasmid construction and yeast transformation

Since the experimental procedures for IL-1β and HSA were identical, we will focus on IL-1β for brevity. All primers used were designed for seamless cloning and are listed in Table S1. All plasmids used in this study are listed in Table S2.

The *Il-1β* gene was codon optimized and synthesized by BGI Inc. (Shenzhen, China) with a 6HIS tag at its N-terminus (Table S3). pKLAC1 vector segment was achieved by amplifying the MCS flanking sequence. pKLAC1-IL-1β was constructed as the IL-1β secretion plasmid using the α-mating signal peptide and as the backbone vector of other plasmids.

To construct YSD strains with different anchors, four commonly used GPI-CWPs (α-agglutinin, Sed1, Cwp2, and C-terminal 428 amino acids of Flot1) encoded by *S. cerevisiae* genome were chosen (accession numbers in Table S3). Their coding sequences, excluding signal peptides, were amplified by PCR and assembled into the pKLAC1-IL-1β vector using the ABclonal MultiF Seamless Assembly Mix kit (ABclonal Inc., Wuhan, China). Unless explicitly stated, all constructs used the α-mating factor from the pKLAC1 vector as a signal peptide. The resulting recombinant plasmids were named pKLAC1-IL-1β-α-agglutinin, pKLAC1-IL-1β-Sed1, pKLAC1-IL-1β-Cwp2, and pKLAC1-IL-1β-Flot1, respectively (Fig. 1a).

For constructing YSD strains with distinct signal peptides, five signal peptides (SP5, SP8, SP14, SP16, and SP26) were randomly chosen from a secretion element library preserved in our lab (sequences in Table S3). These signal peptides were incorporated into pKLAC1-IL-1β-Sed1 by replacing α-mating factor, resulting in five constructs named pKLAC1-SPn-IL-1β-Sed1.

To construct secretory strains, the anchor sequences were removed from the corresponding YSD plasmids, resulting in constructs named pKLAC1-SPn-IL-1β.

All plasmids were then linearized with S*ac* II and transformed into *K. lactis* GG799 competent cells. This process allows for single or tandem integrations of the DNA segment

into the LAC4 locus of *K. lactis* genome via single crossover events. Colony PCR was performed to confirm successful integration. Finally, the recombinant *K. lactis* strains were cultured and induced for protein expression in YPG medium for 72 h, following the manufacturer's instructions from the NEB #E1000S kit.

Immunofluorescence labeling and flow cytometry for detection and sorting of YSD cells

Induced cells were collected and washed with phosphate-buffered saline (PBS, pH 7.0). Pellets were resuspended in a 1:10 dilution of PBS containing 10 mg/mL bovine serum albumin (BSA). Mouse anti-6HIS tag primary antibody (GenScript, Nanjing, China) was added at a 1:100 dilution and incubated with the cells overnight at 4 °C or for 1 h at 30 °C on a shaker. After incubation, cells were harvested, washed with PBS, and incubated with a 1:500 dilution of goat anti-mouse IgG H + L secondary antibody labeled with Alexa Fluor 488 (ABclonal, Wuhan, China) for 1 h at 30 °C. Finally, cells were washed with PBS, adjusted to an optical density (OD 600) of 0.3, and analyzed by flow cytometry (Fortessa X-20, Becton, Dickinson and Company, USA) using 488-nm excitation and 520-nm emission wavelengths. GG799 transformed with a linearized pKLAC1 segment was used as a negative control to eliminate autofluorescence. Cells of suitable size were selected for fluorescence analysis to mitigate the effects of impurities. The obtained results were imported into the FlowJo software for data analysis. For cell sorting, a FACSAria Fusion (BD Biosciences, USA) flow cytometer was used to isolate cells exhibiting the desired fluorescence intensity. Cells with proper fluorescence intensity were sorted and cultured in YPG medium in 96-well microplates for further verification.

Fluorescence microscopy and laser scanning confocal microscopy

Following immunofluorescence labeling, YSD cells were visualized using fluorescence microscopy. A fluorescence microscope (DM5000B, Leica) equipped with 488-nm excitation and 520-nm emission was used to detect green fluorescence of YSD cells. For higher resolution and detailed subcellular localization observation of individual cells, laser scanning confocal microscopy was performed using a Leica TCS SP5 II system with 488-nm excitation.

Quantitative analysis of TP copy numbers and real-time PCR

Single-copy clones were identified using PCR with p1/p2 and p2/p3 primers following the protocol outlined in the NEB #E1000S kit. Absolute quantification of *IL-1β* multi-copies in recombinant *K. lactis* strains was performed using real-time PCR. Genomic DNA was isolated from cell pellets using a commercial kit (GENEWIZ, Suzhou, China). pUC19-GAPDH-AMDS was constructed as the plasmid standard. The *Gapdh* gene served as the internal reference gene during the PCR process, and the copy numbers of *Amds* were used to represent those of TP gene, as they were always integrated simultaneously. Following tenfold serial dilutions of both samples and plasmids, *Gapdh* and *Amds* were amplified using an ABI 7500 FAST system (Thermo, Finland). To ensure accuracy, each sample was analyzed in triplicate under sterile conditions.

Detection of heterologous TP secretory levels

Secretory TP levels were quantified using Western blot analysis. In detail, recombinant strains were cultured and induced in YPG medium for 72 h. Supernatants collected from cultures with equal cell count were subjected to SDS-PAGE. Proteins in the gel were subsequently transferred onto a PVDF membrane. After blocking with 5% nonfat milk at room temperature for 1 h, the membrane was probed with an anti-6HIS tag antibody (1:3,000, Genscript). Unbound antibody was rinsed off, and the membrane was probed with a horseradish peroxidase (HRP)–conjugated goat anti-mouse secondary antibody (1:5,000, Genscript). Protein bands were visualized using enhanced chemiluminescence detection with the Amersham ECL system. Films were exposed for an appropriate time and analyzed using ImageJ software. The level of cell lysis was checked by detecting the intracellular GAPDH with a corresponding antibody on the same membranes.

Plasma mutagenesis and sorting of YSD mutants

YSD cells displaying Sed1-anchored IL-1β were cultured in YPD medium for 15 h to reach the mid-logarithmic growth phase. Subsequently, cell suspension samples were subjected to mutagenesis using Atmospheric and Room Temperature Plasma (ARTP) technology, with an ion beam at 120 W for 0-150 s. Properly diluted cells were then spread on plates to determine the mortality rate. The treated cell samples with a proper mortality rate were cultured and induced for Sed1-IL-1β expression in YPG medium at 30 °C for 72 h. After immunofluorescence labeling, cells with higher fluorescence intensity, indicating higher IL-1β expression, were sorted and cultured in YPG medium in 96-well microplates for further verification. Wild-type cells displaying IL-1β served as the control throughout the experiment.

Verification of improved mutants

The displayed IL-1β-Sed1 protein was extracted from the cell wall and compared between the wild type and an improved mutant. After 72 h of induction, cells were collected and washed using 1.2 M sorbitol solution buffered with 0.1 M sodium phosphate, pH 6.5. Subsequently, the cell pellets were incubated with 0.2% β-mercaptoethanol (ME) for 20 min at room temperature. Following the removal of ME, cell pellets were incubated with lyticase in the above buffer at 30 °C for 2 h. The supernatant was subsequently collected for Western blot analysis.

Results

Evaluating the effectiveness of surface display and anchor selection in *K. lactis*

To confirm successful surface display of IL-1β on *K. lactis*, we employed two approaches: flow cytometry analysis of YSD cells labeled by indirect immunofluorescence, and fluorescence microscopy observation. First, YSD strains harboring each of the four anchors were labeled with an anti-6His antibody and analyzed by flow cytometry. Compared to the negative control, all four strains exhibited distinct increases in fluorescence intensity, indicating the ability of all four anchors to display IL-1β on *K. lactis* surface (Fig. 2). To further verify the cell surface localization of IL-1β, fluorescence microscopy and confocal microscopy were employed for observation. The IL-1β-Sed1 strain exhibited strong green fluorescence upon excitation at 488 nm, while the negative control remained non-fluorescent (Fig. 3a). Confocal microscopy revealed that the green fluorescence originated from the cell periphery of the IL-1β-Sed1 display strain (Fig. 3b), solidifying the successful surface display mediated by the Sed1 anchor. Strains utilizing the other three anchors exhibited weak and barely detectable fluorescence slightly above background levels, indicating weak display of IL-1β (data not shown).

Based on the results from both flow cytometry and microscopy, the strain using Sed1 as the anchor consistently exhibited the strongest fluorescence signal, indicating the highest display capacity. The sequence of this cassette is listed in Table S3. Consistent results were obtained in a separate experiment with HSA as a TP, in which the Sed1

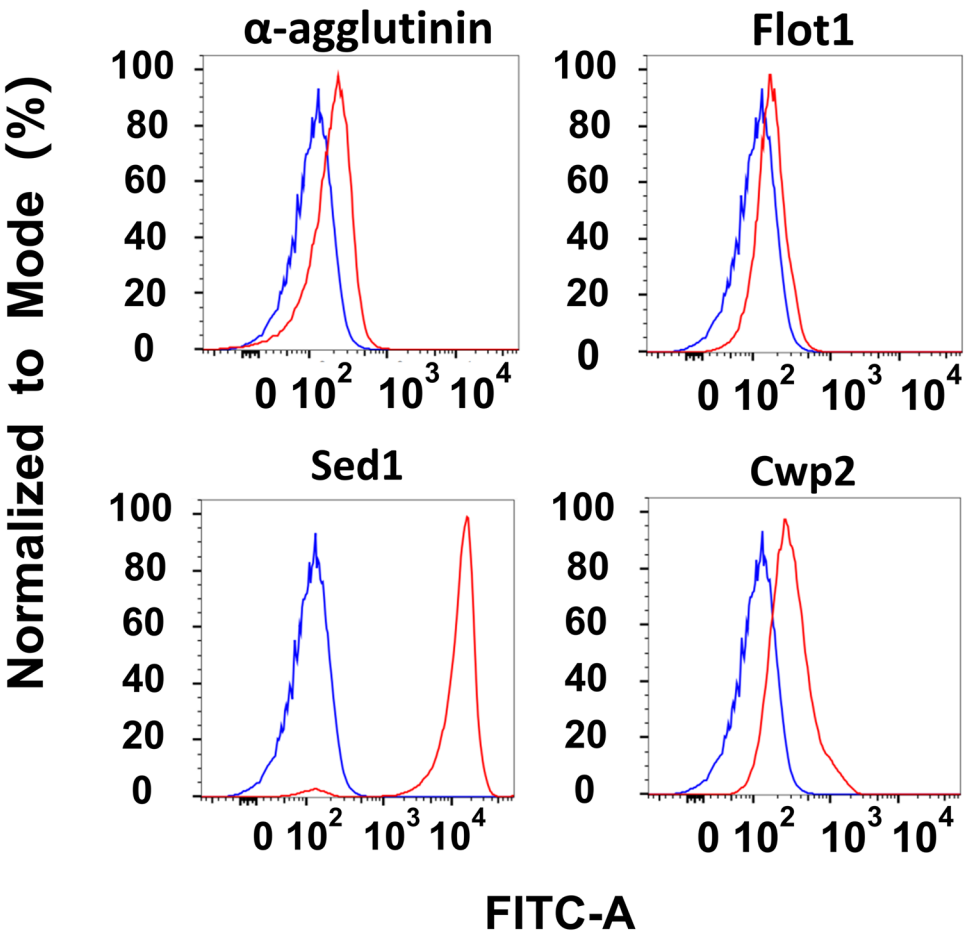

Fig. 2 Flow cytometry analysis and comparison of YSD strains. The display levels are compared between YSD strains with α-agglutinin, Flot1, Sed1, or Cwp2 as an anchor and negative control strain lack of an anchor, respectively. The horizontal axis represents fluorescence signal intensity and the vertical axis represents the cell counts. YSD strains and negative control strains are represented by red and blue peaks, respectively

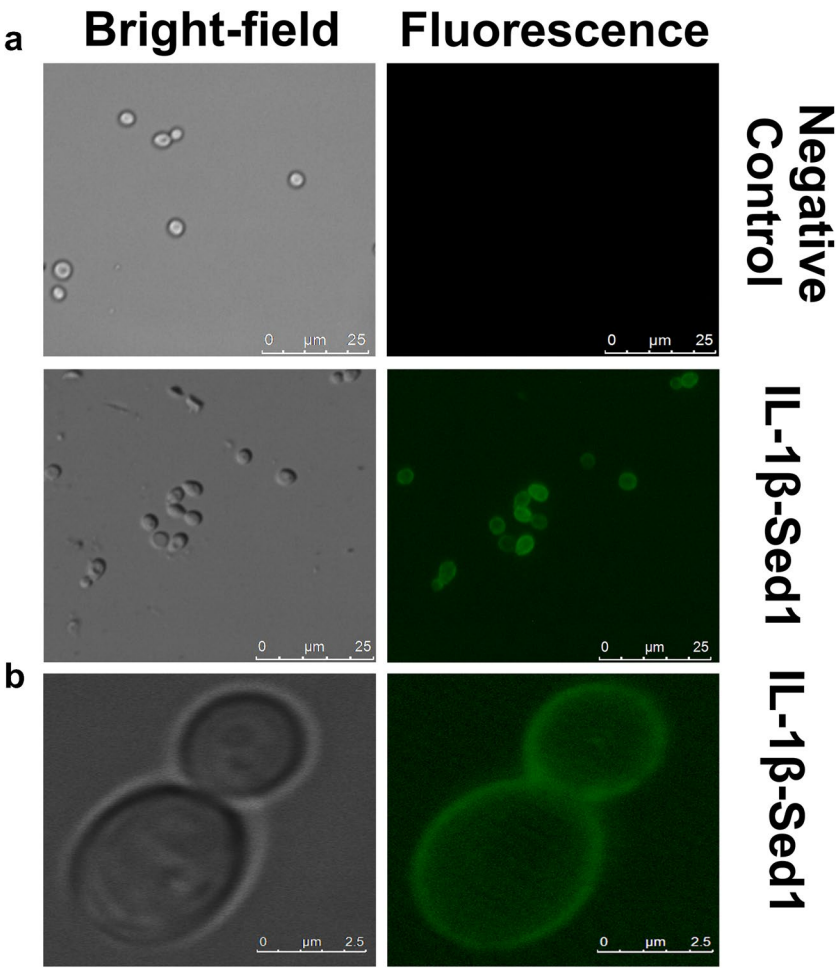

Fig. 3 Immunofluorescence micrographs of YSD strains. **a** Fluorescence microscopy observation of YSD strains expression IL-1β-Sed1 and negative control strains without anchored IL-1β. **b** Confocal microscopy observations of the above strains. Scale bars in figures of fluorescence microscopy and confocal microscopy represent 25 μm and 2.5 μm, respectively

strain also showed the highest fluorescence among all four anchors (Fig. S1).

These observations demonstrate the effectiveness of the YSD system established in this study for displaying TPs in *K. lactis*. Among the four anchors tested, Sed1 consistently exhibited the highest display efficiency. Therefore, Sed1 was selected as the anchor for all subsequent experiments.

Correlation of display and secretion levels under varying expression elements

To investigate if displayed protein levels in *K. lactis* YSD system could accurately reflect secretion levels when expression elements change, we manipulated gene dosage, a simpler alternative to traditional expression element modifications. We detected and compared IL-1β in recombinant YSD and secretory strains with varying *Il-1β* gene dosages, achieved through automatic multiple-integrating events.

We used FACS to sort dozens of YSD strains exhibiting distinct fluorescence intensities. Subsequently, real-time PCR was employed to quantify the integrated copy number of the *Il-1β-Sed1* gene in these strains (Fig. S2). Our results demonstrated a positive correlation between fluorescence intensity of displayed Il-1β and integrated copy number of the *Il-1β* gene, within the range of one to four copies detected (Fig. 4a). Western blot and real-time PCR analysis of secretory strains revealed a similar trend (Fig. 4b). The secretion amount of IL-1β gradually increased as the copy number increased (Fig. 4b). These results indicate that display and secretion levels keep consistent trends under varying expression levels. Intracellular GAPDH could not be probed on the western blot membrane, indicating no obvious cell lysis.

Correlation of display and secretion levels under varying secretion elements

To further verify whether display and secretion are consistently affected by secretion elements, signal peptides were chosen as a model of genetic secretion elements.

Flow cytometry analysis revealed that the strain harboring SP16 exhibited the strongest fluorescence intensity, indicating SP16 facilitated the most efficient display of IL-1β. Meanwhile, SP26 and SP5 had similar moderate

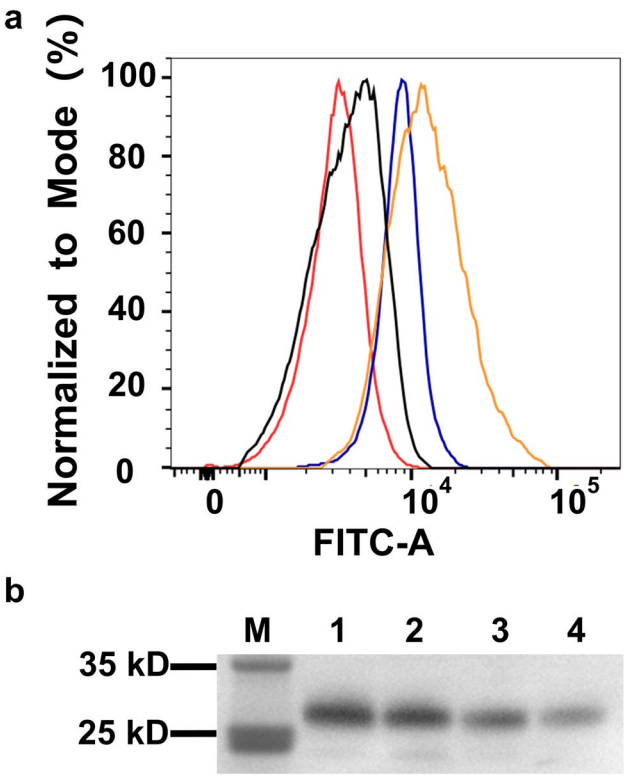

Fig. 4 The protein levels displayed by YSD strains are in accordance with those secreted by the secretory strains, as proved by strains with different gene dosages. **a** Flow cytometry analysis of IL-1β levels displayed by YSD strains with different *sed1* copy numbers. Red, black, blue, and orange peaks represent YSD strains with one, two, three, and four copies of *Il-1β-sed1*, respectively. **b** Western blot analysis of the IL-1β levels secreted by IL-1β secretory strains with different copy numbers. Lane M: protein marker; lanes 1–4: secretory strains with four, three, two, and one copy number of *Il-1β*

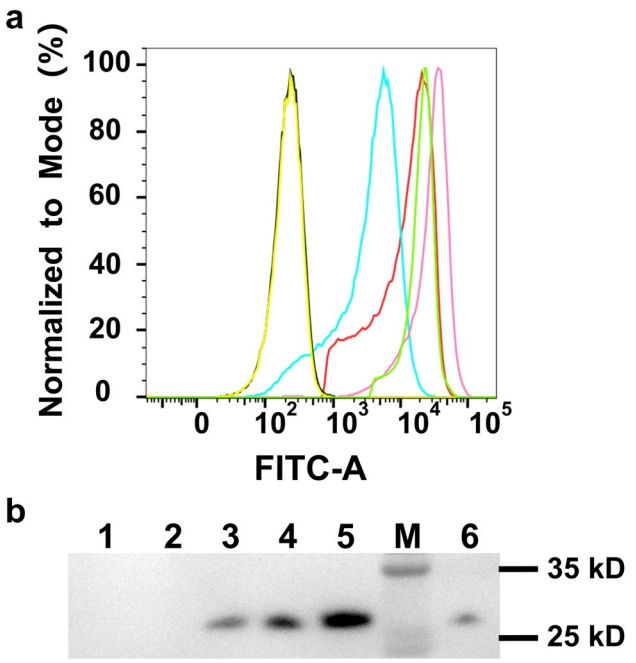

Fig. 5 IL-1β with different signal peptides are displayed or secreted in a consistent level. **a** Flow cytometry analysis of YSD strains harboring various IL-1β expression cassettes with different signal peptides. Red, black, yellow, pink, green, and blue peaks represent IL-1β expression cassettes with SP5, SP8, SP14, SP16, SP26, α-mating, respectively. **b** Western blot analysis of the IL-1β levels secreted by using the above signal peptides. Lanes 1–5: IL-1β levels by secretory strains with SP8, SP14, SP5, SP26, and SP16 as signal peptides; lane M: protein markers; lane 6: IL-1β levels by secreted strains with α-mating factor from pKLAC1 plasmid vector as the positive control

display efficiencies, still outperforming the α factor signal peptide. SP14 and SP8 showed no detectable surface display (Fig. 5a). Consistent results were observed for the corresponding secretory strains analyzed by western blot (Fig. 5b). The protein levels of secreted IL-1β mirrored the order of signal peptide strengths observed in the display analysis, indicating that display and secretory levels are equally affected by secretion elements.

HTS in plasma-induced random mutagenesis library using the developed YSD system

Given the consistent influence of genetic elements on both displayed and secreted protein levels, we hypothesized that displayed levels could reliably reflect a strain's secretory capacity. Based on this premise, we aimed to utilize this YSD system as a HTS method to identify mutants with improved IL-1β secretion from a random mutagenesis library generated using ARTP technique.

The mortality of cells increased with the duration of ARTP treatment (Fig. 6a). A treatment duration of 90 s, resulting in a lethality more than 80%, was chosen as the optimal time. Figure 6b demonstrates that the majority of ARTP-treated cells exhibited fluorescence intensities comparable to the wild type. However, a small population displayed higher fluorescence intensities. Cells within the black box region in Fig. 6b were sorted by FACS, cultured, and analyzed using immunofluorescence labeling and flow cytometry. This process successfully identified dozens of mutants with higher fluorescence intensity, one of which, named M9, was significantly distinct (Fig. 6c). Western blot analysis of Sed1-IL-1β extracted from the cell wall revealed smear bands, indicating the glycosylated status of Sed1 (Shimoi et al. 1998). The intensity of the Sed1-IL-1β bands from mutant M9 was significantly higher than that from the wild-type strain, further confirming the improved yield of the mutant (Fig. 6d). Sequencing and qPCR results excluded mutations and the dosage variation within the IL-1β display cassette itself. The results showed that M9 possessed enhanced display capacity, suggesting an enhanced secretory efficiency of IL-1β, potentially due to an improved secretory

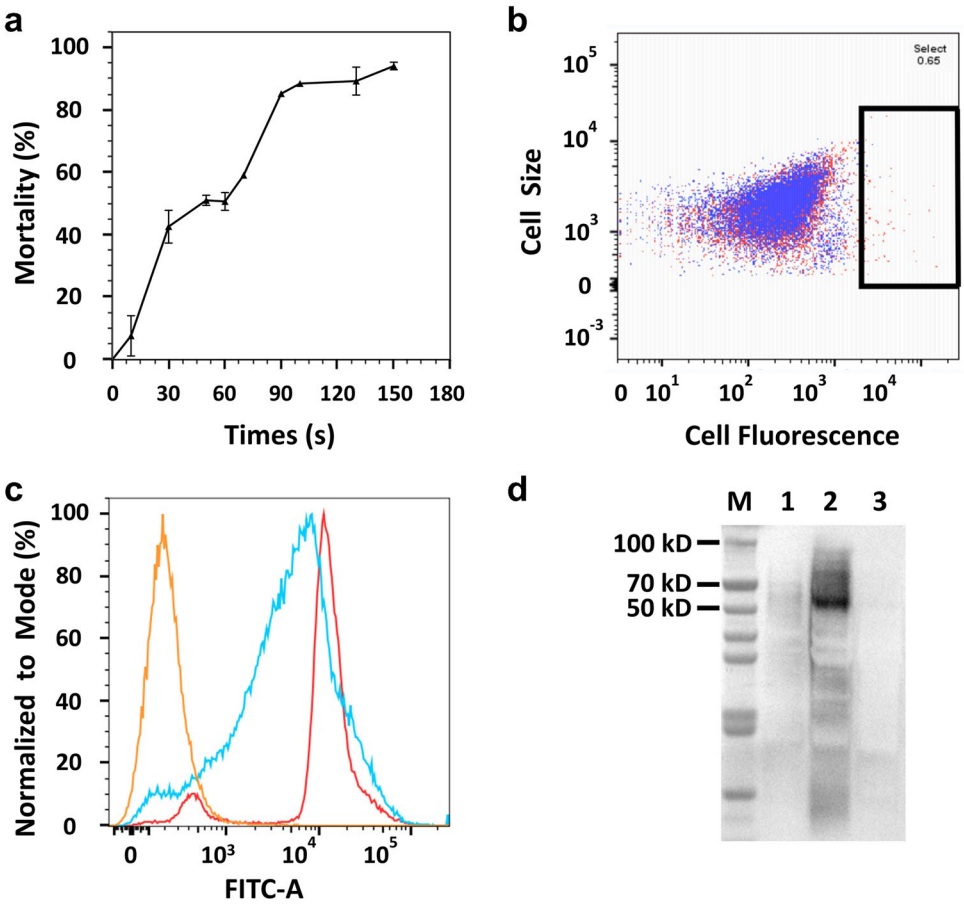

Fig. 6 HTS utilizing the developed YSD system. **a** Lethality curve of the YSD strain after different duration of ARTP treatment. **b** FACS of plasma-induced random mutagenesis library. The wild-type and the mutant strains are depicted in blue and red, respectively. The mutant strains enclosed within a black box were selected for further verification. **c** Flow cytometric analysis of the selected strains. Blue, red, and orange peaks represent the wild type, mutant M9 and negative control, respectively. **d** Western blot analysis of IL-1β-Sed1 extracted from the cell wall. Lane M: protein marker; lanes 1–3: wild type, mutant M9, negative control

chassis strain. Genome sequencing of the optimal mutants will be performed after several rounds of ARTP treatment. This outcome demonstrates the feasibility of utilizing YSD technology developed in this study as a HTS method for identifying strains with elevated secretion capacity.

Discussion

This study established a YSD system in *K. lactis* capable of effectively displaying diverse TPs. We demonstrated a remarkable correlation between protein display levels and secretion efficiency, suggesting that display levels can serve as a reliable indicator of a strain's secretory capacity. The YSD system proved effective in identifying genetic elements that enhance secretion and in screening for high-secretory strains producing recombinant non-enzymatic proteins.

The expression cassette of the YSD system comprises of three essential components: an anchor protein tethering the TP, a linker connecting the anchor and TP, and a detection tag. In this study, we systematically compared four anchors and analyzed their synergistic interactions with other components.

Among the four potential anchors compared, Sed1 demonstrated the most effective display of TPs in *K. lactis*. This finding aligns with previous studies in other yeasts, such as *S. cerevisiae* (Van der Vaart et al. 1997), *Candida tropicalis* (Wang et al. 2023), and *Y. lipolytica* (Yuzbashev et al. 2011), where Sed1 has been shown to be a superior anchor protein. The molecular size of Sed1 is likely a contributing factor to its effectiveness. Larger anchors like α-agglutinin can lead to TPs entrapped within the cell wall, hindering their interaction with large substrates. In contrast, smaller anchors like Cwp2 allow for greater penetration of the cell wall, enabling the displayed proteins to interact with substrates of various sizes (Van der Vaart et al. 1997). Another study also observed a significant reduction in enzymatic activity against large substrates when using α-agglutinin as an anchor (Schreuder et al. 1996). From another point of view, in contrast to α-agglutinin which is primarily localized on the internal surface of the cell wall, Sed1 is predominantly found on the external surface (Inokuma et al. 2019). This localization facilitates the detection of displayed TPs, confirming Sed1's suitability as an optimal anchor.

An ideal anchor should be versatile, effectively displaying a wide range of TPs with diverse properties. It is commonly considered the size and structure of TPs can influence

display efficiency. For example, Tang et al. found that the bulky cellulolytic enzyme BGL1 (96 kD) was undetectable by FACS in their YSD system, while the smaller CelA endoglucanase (52kD) was displayed effectively (Tang et al. 2017). In this study, we further demonstrated the versatility of the Sed1 anchor by successfully displaying HSA as a second large and complex model TP. Although HSA (66 kD) display efficiency was lower compared to the smaller IL-1β (17 kD), Sed1's ability to display both small and large proteins highlights its potential as a universal anchor in the *K. lactis* YSD system (Fig. S1). We hypothesized that the challenge in displaying HSA mainly arises from its intricate structure containing 17 disulfide bonds. Given its demonstrated effectiveness with diverse TPs and its superior performance compared to other tested anchors, we propose Sed1 as a promising candidate for a universal anchor in the *K. lactis* YSD system.

The length of the linker between the anchor and TP can also influence display efficiency. Longer linkers, often composed of Ser/Thr-rich sequences or $(Gly_4Ser)_3$ repeats, are considered necessary to maintain TP conformation and accessibility (Washida et al. 2001; Zhang et al. 2019). For example, a YSD system incorporating a 17-amino acid linker, composed of flexible Gly/Ser repeats, was proved to be the most effective (Yang et al. 2019). While such linkers can be beneficial, our study found that a shorter and simpler linker consisting of only five amino acids (Gly_4Ser) was sufficient. This shorter linker, without repetitive sequences, offers obvious advantages including reduced time and costs for genetic construction and minimal impact on TP structures.

A 6HIS tag was introduced at the N-terminus of the TP as a detection tag for this YSD system. Detection was carried out using indirect immunofluorescence labeling of the 6HIS tag, followed by flow cytometric analysis. We proposed this approach as a general solution for detecting the display levels of non-enzymatic proteins. While traditional YSD detection methods often rely on enzyme assays or fluorescent protein measurements, for non-enzymatic and non-fluorescent proteins, immunofluorescence antibodies are typically required (Kim et al. 2006; Starwalt et al. 2003). It is a time-consuming and costly task to prepare a specific antibody for each specific TP. The commonly used 6HIS tag offers a more versatile solution, as it is known to have minimal impact on protein expression and translocation processes. An immunofluorescence antibody against the 6HIS tag can be used as a universal reagent for detecting all displayed non-enzymatic proteins. Additionally, for applications like immobilized enzymes, YSD cells can be recycled using reusable Ni magnetic beads. Previous studies have also occasionally utilized V5 or c-myc tags for YSD detection (Rakestraw et al. 2006; Wentz and Shusta 2007; Yang et al. 2019). These cells can only be collected by disposable antibody-modified magnetic beads, which are more costly than Ni magnetic beads. From these perspectives, the 6HIS tag offers a reliable and cost-effective solution for both detection and cell collection in the YSD system.

Therefore, we can conclude that the YSD system developed in our study incorporates three key elements described above, making it a cost-effective and versatile platform for displaying TPs in *K. lactis*. The YSD technique has the potential to enhance various applications of *K. lactis*, including vaccine and antibody development, library screening, bioconversion of contaminants, and biosorption of heavy metals. The primary objective of this study was to utilize this YSD system as a universal HTS method specifically tailored for assessing the secretory levels of non-enzymatic proteins.

As aforementioned, theoretically genetic elements should influence displayed and secreted TP levels consistently. Consequently, elements promoting higher display are expected to enhance secretion. However, occasional discordances have also been observed, potentially due to the anchor's impact on expression or translocation processes (Piatesi et al. 2006; Wentz and Shusta 2007). These discrepancies could lead to missed identification or false positives when using this YSD system for HTS. Therefore, to ensure reliable screening for production-enhancing genetic elements, it is imperative to assess their consistent effects on both display and secretion in this system. We compared trends in displayed and secreted TP levels to evaluate their consistency when representative expression or translocation elements were altered. Our results demonstrated a strong correlation between displayed and secreted TPs, suggesting that display levels in this YSD system can serve as a reliable indicator of secretory capacity.

High levels of secreted proteins are the premise of large-scale industrial production. However, targeting the non-enzymatic proteins, the universal and efficient HTS methods for obtaining the hypersecretory strains or identifying secretion-enhancing genetic elements are limited. Traditional approaches often involve costly techniques like ELISA or droplet microfluidics, and require a unique experimental design for each specific protein (Ito et al. 2022; Lee et al. 2022). Meanwhile, most existing YSD-based HTS methods are designed for enzymes and rely on activity assays for detection (Bae et al. 2015; Tang et al. 2017; Yang et al. 2019). The immunofluorescence labelling-dependent YSD systems are typically used for antibody screening or engineering (Mustafa et al. 2024; Oh et al. 2020). This study introduces a YSD system in *K. lactis* specifically designed for HTS of strains with enhanced secretion of non-enzymatic proteins, which constitute a significant portion of food and pharmaceutical proteins. This YSD system can be used for rapid characterization and comparison of secretory strains and genetic elements in large quantities, as well as for the HTS of large random mutagenesis libraries. We believe this *K. lactis* YSD system could significantly accelerate the

screening process for identifying strains that secrete high levels of non-enzymatic proteins.

In conclusion, we have successfully established a robust YSD system in *K. lactis*. The strong correlation between protein display levels and secretion efficiency in this system demonstrates its reliability as a universal HTS method for strains producing high levels of non-enzymatic proteins. We believe this YSD system could significantly contribute to the large-scale production of food and pharmaceutical proteins in various industries.

Supplementary Information The online version contains supplementary material available at https://doi.org/10.1007/s00253-024-13342-9.

Author contribution YZ conceived and designed research. JA, NS, and WL conducted experiments. YN and QL guided the methods and analyzed data. JA and YZ wrote the manuscript. YZ and JJ acquired the funding and supervised the project. All authors read and approved the manuscript.

Funding This work was supported by Tianjin Synthetic Biotechnology Innovation Capacity Improvement Project (TSBICIP-KJGG-013) to YZ and the National Natural Science Foundation of China (Grant No. U23A20143 and 32070031) to JJ.

Data availability The datasets generated during and/or analyzed during the current study are available from the corresponding author on reasonable request.

Declarations

Ethics approval This article does not contain any studies with human participants or animals performed by any of the authors.

Conflict of interest The authors declare no competing interests.

References

Almeida CM, Gomes D, Faro C, Simões I (2015) Engineering a cardosin B-derived rennet for sheep and goat cheese manufacture. Appl Microbiol Biotechnol 99(1):269–281

Bae JH, Sung BH, Kim HJ, Park SH, Lim KM, Kim MJ, Lee CR, Sohn JH (2015) An efficient genome-wide fusion partner screening system for secretion of recombinant proteins in yeast. Sci Rep 5:12229

Bao WG, Fukuhara H (2001) Secretion of human proteins from yeast: stimulation by duplication of polyubiquitin and protein disulfide isomerase genes in *Kluyveromyces lactis*. Gene 272(1–2):103–110

Cheon SA, Jung J, Choo JH, Oh DB, Kang HA (2014) Characterization of putative glycosylphosphatidylinositol-anchoring motifs for surface display in the methylotrophic yeast *Hansenula polymorpha*. Biotechnol Lett 36:2085–2094

Cong L, Tian Y, Huo Z, Xu W, Hou C, Shi W, Wang W, Liang C, Xu S (2022) Single-cell VEGF analysis by fluorescence imaging-microfluidic droplet platform: an immunosandwich strategy on the cell surface. Anal Chem 94(17):6591–6598

Feng Y, Zhang B, Zhang Y, Hiroshi F (1997) Secretory expression of porcine insulin precursor in *Kluyveromyces lactis* and its conversion into human insulin. Acta Biochim Biophys Sin 29(2):129–134

Freitas MdFMd, Hortêncio LC, Albuquerque TLd, Rocha MVP, Gonçalves LRB (2020) Simultaneous hydrolysis of cheese whey and lactulose production catalyzed by β-galactosidase from *Kluyveromyces lactis* NRRL Y1564. Bioprocess Biosyst Eng 43(4):711–722

Fukuhara H (2006) *Kluyveromyces lactis*- a retrospective. FEMS Yeast Res 6:323–324

Hua Z, Liang X, Zhu D (1994) Expression and purification of a truncated macrophage colony stimulating factor in *Kluyveromyces lactis*. Biochem Mol Biol Int 34(2):419–427

Idiris A, Tohda H, Kumagai H, Takegawa K (2010) Engineering of protein secretion in yeast: strategies and impact on protein production. Appl Microbiol Biotechnol 86:403–417

Inokuma K, Kurono H, Haan Rd, van Zyl WH, Hasunuma T, Kondo A (2019) Novel strategy for anchorage position control of GPI-attached proteins in the yeast cell wall using different GPI-anchoring domains. Metab Eng 57:110–117

Ito Y, Ishigami M, Terai G, Nakamura Y, Hashiba N, Nishi T, Nakazawa H, Hasunuma T, Asai K, Umetsu M, Ishii J, Kondo A (2022) A streamlined strain engineering workflow with genome-wide screening detects enhanced protein secretion in *Komagataella phaffii*. Commun Biol 5:561

Kim Y-S, Bhandari R, Cochran RJ, Kuriyan J, Wittrup KD (2006) Directed evolution of the epidermal growth factor receptor extracellular domain for expression in yeast. Proteins 62(4):1026–1035

Kumar L, Gangadharan V, Raghunadha DR, Saikia T, Shah S, Malhotra H, Bapsy P, Singh K, Rao R (2005) Safety and efficacy of an indigenous recombinant interferon-α-2b in patients with chronic myelogenous leukaemia: results of a multicentre trial from India. Natl Med J India 18(2):66–70

Lee MS, Chang YC, Huang HY, Hsu W (2022) Single-type reporter multiplexing with a single droplet through bead-based digital microfluidics. J Pharmaceut Biomed Anal 219:114877

Legastelois I, Buffin S, Peubez I, Mignon C, Sodoyer R, Werleb B (2017) Non-conventional expression systems for the production of vaccine proteins and immunotherapeutic molecules. Hum Vaccin Immunother 13(4):947–961

Madhavan A, Arun BK, Sindhu R, Krishnamoorthy J, Reshmy R, Sirohi R, Pugazhendi A, Awasthi KM, Szakacs G, Binod P (2021) Customized yeast cell factories for biopharmaceuticals: from cell engineering to process scale up. Microb Cell Fact 20:124

Musch E, Malek M, Eick H, Chrissafidou A (2004) Successful application of highly purified natural interferon α (multiferon) in a chronic hepatitis C patient resistant to preceeding treatment approaches. Hepatogastroenterol 51(59):1476–1479

Mustafa MI, Alzebair AA, Mohammed A (2024) Development of recombinant antibody by yeast surface display technology. Curr Res Pharmacol Drug Discov 6:100174

Oh EJ, Liu R, Liang L, Freed EF, Eckert CA, Gill RT (2020) Multiplex evolution of antibody fragments utilizing a yeast surface display platform. ACS Synth Biol 9(8):2197–2202

Piatesi A, Howland WS, Rakestraw AJ, Renner C, Robson N, Cebon J, Maraskovsky E, Ritter G, Old L, Wittrup DK (2006) Directed evolution for improved secretion of cancer-testis antigen NY-ESO-1 from yeast. Protein Expr Purif 48(2):232–242

Rakestraw JA, Baskaran AR, Wittrup KD (2006) A flow cytometric assay for screening improved heterologous protein secretion in yeast. Biotechnol Prog 22:1200–1208

Robin S, Petrov K, Dintinger T, Kujumdzieva A, Tellier C, Dion M (2003) Comparison of three microbial hosts for the expression of an active catalytic ScFv. Mol Immunol 39(12):729–738

Rodicio R, Heinisch JJ (2013) Yeast on the milky way: genetics, physiology and biotechnology of *Kluyveromyces lactis*. Yeast 30:165–177

Rodicio R, Schmitz H-P, Heinisch JJ (2022) Genetic and physiological characterization of fructose-1,6-bisphosphate aldolase and glyceraldehyde-3-phosphate dehydrogenase in the crabtree-negative yeast *Kluyveromyces lactis*. Int J Mol Sci 23(2):772

Sampaio FC, Faria JTd, Silva MFd, Oliveira RPdS, Converti A (2020) Cheese whey permeate fermentation by *Kluyveromyces lactis*: a combined approach to wastewater treatment and bioethanol production. Environ Technol 41(24):3210–3218

Schreuder MP, Mooren AT, Toschka HY, Verrips CT, Klis FM (1996) Immobilizing proteins on the surface of yeast cells. Trends Biotechnol 14:115–120

Shimoi H, Kitagaki H, Ohmori H, Iimura Y, Ito K (1998) Sed1p is a major cell wall protein of Saccharomyces cerevisiae in the stationary phase and is involved in lytic enzyme resistance. J Bacteriol 180(13):3381–3387

Shusta EV, Kieke MC, Parke E, Kranz DM, Wittrup KD (1999) Yeast polypeptide fusion surface display levels predict thermal stability and soluble secretion Eefficiency. J Mol Biol 292:949–956

Spohner SC, Schaum V, Quitmann H, Czermak P (2016) *Kluyveromyces lactis*: an emerging tool in biotechnology. J Biotechnol 222:104–116

Starwalt ES, Masteller LE, Bluestone AJ, Kranz MD (2003) Directed evolution of a single-chain class II MHC product by yeast display. Protein Eng Des Sel 16(2):147–156

Stucki A, Vallapurackal J, Ward TR, Dittrich PS (2021) Droplet microfluidics and directed evolution of enzymes: an intertwined journey. Angew Chem Int Ed Engl 60(46):24368–24387

Swennen D, Paul M, Vernis L, Beckerich J, Fournier A, Gaillardin C (2002) Secretion of active anti-Ras single-chain Fv antibody by the yeasts *Yarrowia lipolytica* and *Kluyveromyces lactis*. Microbiology 148(1):41–50

Tanaka T, Kondo A (2014) Cell-surface display of enzymes by the yeast *Saccharomyces cerevisiae* for synthetic biology. FEMS Yeast Res 15(1):1–9

Tang H, Song M, He Y, Wang J, Wang S, Shen Y, Hou J, Bao X (2017) Engineering vesicle trafficking improves the extracellular activity and surface display efficiency of cellulases in *Saccharomyces cerevisiae*. Biotechnol Biofuels 10:53–65

Tang S, Tao J, Li Y (2024) Challenges and solutions for the downstream purification of therapeutic proteins. Antib Ther 7(1):1–12

Teymennet-Ramírez V, Martínez-Morales F, Trejo-Hernández R (2022) Yeast surface display system: strategies for improvement and biotechnological applications. Front Bioeng Biotechnol 9:794742

Uccelletti D, Jaco DA, Farina F, Mancini P, Augusti-Tocco G, Biagioni S, Palleschi C (2002) Cell surface expression of a GPI-anchored form of mouse acetylcholinesterase in Klpmr1Delta cells of *Kluyveromyces lactis*. Biochem Biophys Res Commun 298(4):559–565

van den Dungen MW, Boer R, Wilms LC, Efimova Y, Abbas HE (2021) The safety of a *Kluyveromyces lactis* strain lineage for enzyme production. Regul Toxicol Pharmacol 126:105027

Van der Vaart JM, Biesebeke RT, Chapman JW, Toschka HY, Klis FM, Verrips CT (1997) Comparison of cell wall proteins of *Saccharomyces cerevisiae* as anchors for cell surface expression of heterologous proteins. Appl Environ Microbiol 63(2):615–620

van Ooyen JJ, Dekker P, Huang M, Olsthoorn MA, Jacobs I, Colussi A, Taron H (2006) Heterologous protein production in the yeast *Kluyveromyces lactis*. FEMS Yeast Res 6:381–392

Wang L, Wang N, Zhang W, Cheng X, Yan Z, Shao G, Wang X, Wang R, Fu C (2022) Therapeutic peptides: current applications and future directions. Signal Transduct Target Ther 7:48

Wang T, Zhang H, Li M, Zheng J, Xia Y, Yang H, Shen W, Chen X (2023) Development of surface displaying system for heterologous protein expression in *Candida tropicalis*. Syst Microbiol Biomanufacturing 3:298–311

Washida M, Takahashi S, Ueda M, Tanaka A (2001) Spacer-mediated display of active lipase on the yeast cell surface. Appl Microbiol Biotechnol 56(5–6):681–686

Wentz AE, Shusta EV (2007) A novel high-throughput screen reveals yeast genes that increase secretion of heterologous proteins. Appl Environ Microbiol 73(4):1189–1198

Yang H, Liu L, Xu F (2016) The promises and challenges of fusion constructs in protein biochemistry and enzymology. Appl Microbiol Biotechnol 100(19):8273–8281

Yang X, Tang H, Song M, Shen Y, Hou J, Bao X (2019) Development of novel surface display platforms for anchoring heterologous proteins in *Saccharomyces cerevisiae*. Microb Cell Fact 18(1):85

Yuzbashev EY, Yuzbashev TV, Laptev IA, Konstantinova TK, Sineoky PS (2011) Efficient cell surface display of Lip2 lipase using C-domains of glycosylphosphatidylinositol-anchored cell wall proteins of *Yarrowia lipolytica*. Appl Microbiol Biotechnol 91:645–654

Zeng Y, Chen E, Zhang X, Li D, Wang Q, Sun Y (2022) Nutritional value and physicochemical characteristics of alternative protein for meat and dairy- a review. Foods 11:3326

Zhang Y, Min Z, Qin Y, Ye DQ, Song YY, Liu YL (2019) Efficient display of *Aspergillus niger* β-Glucosidase on *Saccharomyces cerevisiae* cell wall for aroma enhancement in wine. J Agric Food Chem 67:5169–5176

Zhao N, Xu Y, Wang K, Zheng S (2017) Synthesis of isomalto-oligosaccharides by *Pichia pastoris* displaying the *Aspergillus niger* α-glucosidase. J Agric Food Chem 65:9468–9474